

## 2D ZIF-L(Zn) for Hybrid Copolymerization of Methyl Methacrylate and $\epsilon$ -Caprolactone under Solvent-free Medium

F. Yasmin and M. A. Rahaman\*

Department of Chemistry, Mawlana Bhashani Science and Technology University, Santosh,  
Tangail-1902, Bangladesh

Received 21 March 2023, accepted in final revised form 2 September 2023

### Abstract

Herein, we report the hybrid copolymerization of methyl methacrylate (MMA) and  $\epsilon$ -caprolactone (CL). 2D metal-organic frameworks, ZIF-L as a robust polymerization catalyst, can catalyze this hybrid copolymerization. Though these monomers differ from each other in structure and activity, different characterization techniques ( $^1\text{H-NMR}$ ,  $^{13}\text{C-NMR}$ , GPC, DSC, fractional precipitation techniques) confirm that they form biodegradable block copolymer PMMA-*b*-PCL with high molecular weight (1190 kg/mol). Also, PXRD and SEM results of the recovered ZIF-L reveal that the catalyst ZIF-L is remarkably stable even after a long-time polymerization reaction with no significant loss in activity.

**Keywords:** Zeolitic imidazolite framework; Block copolymer; Methyl methacrylate,  $\epsilon$ -caprolactone.

© 2024 JSR Publications. ISSN: 2070-0237 (Print); 2070-0245 (Online). All rights reserved.  
doi: <http://dx.doi.org/10.3329/jsr.v16i1.65039> J. Sci. Res. **16** (1), 253-264 (2024)

### 1. Introduction

In the last few decades, metal-organic frameworks (MOFs) have represented a novel class of porous materials due to their unique properties like tailorable porosity, high mechanical, chemical, and thermal stability, and large surface area [1]. Because of these fascinating properties, MOFs have been studied for many applications, including gas storage and separation, energy saving and conversion, catalysis, sensors, and biomedicine [2-4]. Structural diversity makes MOFs 1D, 2D, and 3D structures with different properties, and for this, compatible and flexible metallic ions and a variety of types of organic ligands are mainly responsible. And for all of the above, MOFs-related research has become one of the recent fast-growing fields of chemistry and materials.

Zeolitic imidazolite frameworks (ZIFs) are a sub-class of MOFs that incorporates the fascinating features of typical MOFs and zeolite structures and have great attracted in various attractive applications due to their tunable pore size, chemical robustness, and thermal and chemical stability [5-7]. Tetrahedral metallic ions (such as Zn and Co) and imidazolite-based organic ligands mainly form this special class of MOFs. However, in

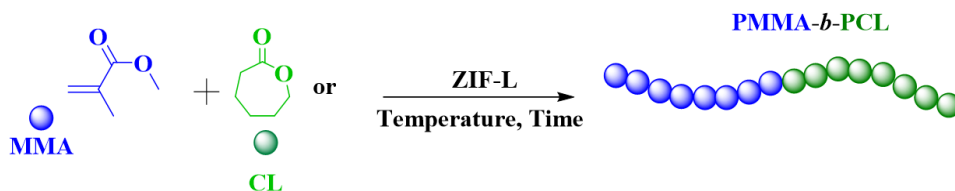
---

\* Corresponding author: [md.arch27@mbstu.ac.bd](mailto:md.arch27@mbstu.ac.bd)

2013, Wang and his team synthesized a new type of 2D ZIF (known as ZIF-L) with a leaf-like structure that has since been able to attract significant attention in a variety of applications, especially due to its porosity, 2D structure, green synthesis process and the Lewis pairs feature [8-10]. This structural morphology of 2D ZIF-L reveals that the ZIF-L's metallic site is more readily available compared to its 3D structure ZIF-8 [11]. Since Lewis pair components have emerged as new types of catalysts for different polymerization reactions, this feature of 2D ZIF-L could create a groundbreaking opportunity for use as catalysts in different polymerization reactions [12].

Synthetic polymers have a vital role in modern life and technology. However, the biostability of most polymers is a major barrier to sustainable development. Hence, bio-stable materials are increasingly shifting to biodegradable materials, especially in biomedical applications [13,14]. Polyester is one of the most researched biodegradable materials in the last three decades [15]. Among poly(ester)s, aliphatic polyesters can be considered as representatives of synthetic biodegradable polymers because they contain both biocompatibility and biodegradability nature and are made from renewable biofeedstock [16].

On the other hand, polyacrylates are widely applied in the biomedical field due to their biocompatible nature, though they are not biodegradable [17]. Therefore, it is highly demandable to convert bio-stable materials into biodegradable for sustainable development. It could be done by creating polymer blends or copolymers with biodegradable polymers better suited for biomedical applications. However, in the case of copolymerization of acrylates (vinyl monomers) with cyclic esters (cyclic monomers), these monomers differ from each other in structure and activity, so they usually follow very different polymerization mechanism, catalysts, and propagation species in their homo-polymer formation [18]. Furthermore, among the copolymers, block copolymers have structural and compositional distinctions from homo- or random copolymers. They consist of two or more independent macromolecular chains and thus possess outstanding properties. In the present study, we report the synthesis of block copolymer from the vinyl monomer, methyl methacrylate (MMA) with cyclic monomer,  $\epsilon$ -caprolactone (CL) such as PMMA-*b*-PCL using 2D ZIF-L as copolymerization catalyst following simple sequential addition method of monomers (Scheme 1).



Scheme 1. Synthesis of block copolymers from acrylates (methyl methacrylate, MMA) and cyclic esters ( $\epsilon$ -caprolactone, CL).

## 2. Experimental

### 2.1. Materials and methods

All the required chemicals and reagents were used in this work by purchasing from various known chemical suppliers such as  $\text{Zn}(\text{NO}_3)_2 \cdot 6\text{H}_2\text{O}$  (>98 %) from Sigma Aldrich, 2-methylimidazole (2-mIm; 99 %), methyl methacrylate (MMA; 99 %), and  $\epsilon$ -caprolactone (CL; 99 %) from Aladdin Chemical Co. Ltd. And, all reagents and solvents were used as received from commercial suppliers without further purification. Before use, MMA was purified at a reduced pressure of 50 °C (at least two times distillation) and used.

### 2.2. Synthesis of ZIF-L

Following the facile and green synthesis procedure (thermal-free and in an aqueous medium), 2D ZIF-L(Zn) with leaf-like structure was synthesized from  $\text{Zn}(\text{NO}_3)_2 \cdot 6\text{H}_2\text{O}$  as the metal source and 2-mIm as the ligand [8,9]. Firstly,  $\text{Zn}(\text{NO}_3)_2 \cdot 6\text{H}_2\text{O}$  (0.595 g, 2 mmol) was dissolved in 40 mL deionized water and sonicated for 20 min. to obtain a homogeneous solution and mark it as solution A. Similarly, 2-mIm (1.32 g, 16 mmol) was dissolved in 40 mL of deionized water and sonicated 20 min to obtain a homogeneous solution and marked as solution B. After that, solution A was added dropwise with solution B under constant stirring. The mixture was stirred at room temperature for 3 h, and after that, the product was collected by repeated centrifugation at 7000 rpm for 5 min, washed with fresh deionized water several times, and finally dried at 80 °C under vacuum overnight.

### 2.3. Analytical and morphological characterization

The structural morphology of ZIF-L was examined using several analytical techniques, including SEM, PXRD, FT-IR, TGA, and nitrogen sorption measurements. The structural morphology of ZIF-L(Zn) was determined with a scanning electron microscope (SEM) from JEOL (JSM-IT300, 0.5–35 kV). The powder X-ray diffraction (PXRD) spectral study of ZIF-L was performed with a Panalytical Empyrean instrument using monochromatic Cu  $K\alpha$  radiation in the  $2\theta$  range of 3° to 60° at a scan rate of 2°/min. Fourier transform infrared spectroscopy (FT-IR) was performed using Bruker Vertex 80V ranging from 4000–400  $\text{cm}^{-1}$ . Thermogravimetric analysis (TGA) was carried out on a Netzsch (STA 449C) instrument (5 °C/min as heating rate) under  $\text{N}_2$  atmosphere (20 mL/min) in the range of 25–800 °C. The surface area and adsorption/desorption isotherm were measured using  $\text{N}_2$  adsorption on Micromeritics ASAP 2020 equipment. For this, the ZIF-L sample was first degassed at 150 °C for 3 h. Also, the amount of acidic and basic sites of ZIF-L was determined with temperature-programmed desorption (TPD) profile of  $\text{NH}_3$  and  $\text{CO}_2$  using Micromeritics chemisorb 2750 Pulse Chemisorption, respectively.

#### 2.4. Copolymerization of MMA with CL

At first, the catalysts (ZIF-L) were activated at 120 °C for 6 h with a temperature rate of 1 °C/min under vacuum. All reactions were performed under an inert atmosphere using standard Schlenk techniques. Specified amounts of activated ZIF-L and purified MMA were charged into a dry shank flask in the nitrogen-flowing inert atmosphere of the glove box. The flask was then sealed carefully and placed in a pre-heated oil bath at 140 °C and heated for 24 h. Then, the purified CL was added to the Schlenk in the inert atmosphere at the glove box, and the mixture was heated for 24 h. After 24 h (total of 48 h), the reaction was terminated by cooling the flask in an ice bath (0 °C). After cooling to ambient temperature and quenching the mixture in the air, the monomer conversion was determined by <sup>1</sup>H-NMR spectroscopy using CDCl<sub>3</sub> as solvent. The remaining polymeric material was then dissolved in THF and filtered to remove the catalyst. Afterward, the polymer was re-precipitated with cold methanol and washed several times with fresh methanol. The resulting material was then dried at 60 °C under vacuum for 24 h and collected as a white solid. However, the polymer was purified further by fractional precipitation.

#### 2.5. Fractional precipitations of the polymers

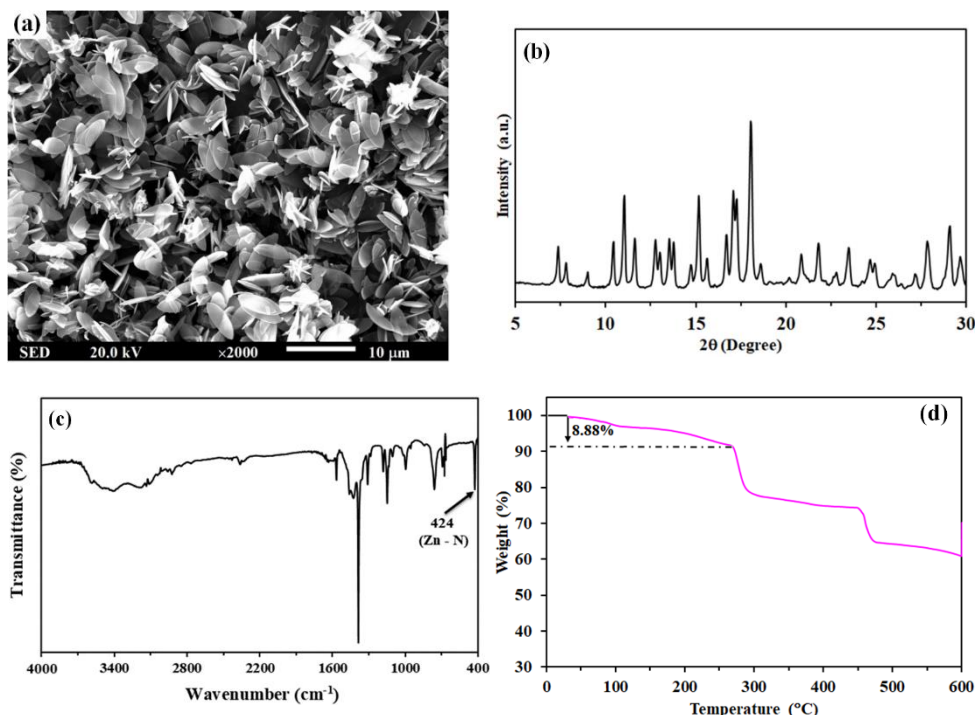
Fractional precipitation of polymer is a technique that provides evidence of the formation of block copolymers. This technique was carried out according to the procedure cited in the literature [19,20]. At first, approximately 0.5 g of the dried polymeric sample was dissolved in 10 mL of THF,  $V_s$ . Methanol was then slowly added (dropwise) into the rapid stirring of these solutions until turbidity occurred,  $V_{n1}$  (The volume of methanol used until the first precipitation was observed). At this stage, the larger molecules precipitate first, and the smaller ones remain in the solution. The solutions were then allowed to decant, and after decantation, methanol was added at the upper portion of the solution for a second fractionation and continued the same procedure until no more precipitation was observed,  $V_{n2}$  (total volume of the methanol used in the precipitation). Using the equation  $\gamma = V_n/V_s$ , the range of gamma values ( $\gamma_1 \sim \gamma_2$ ) for each homo and copolymer is calculated in the range of the precipitation starts and ends. Generally, the gamma values of the block copolymers have been between that of homo PMMA and that of homo PCL. Afterward, the polymer fractions were separated by centrifugation and dried under vacuum at 60 °C for 24 h.

### 3. Results and Discussion

#### 3.1. Structural characterization of ZIF-L

The catalytic activity of any material depends on its structural purity, so, firstly, the pure phase structure of ZIF-L was characterized using various techniques, including SEM, PXRD, FT-IR, TGA, and nitrogen sorption measurements, and the results found were in

good agreement with reported studies. Fig.1(a) demonstrated the morphology of the synthesized ZIF-L, which revealed a leaf-like shape with an average size of around  $5.9 \mu\text{m} \times 2.4 \mu\text{m}$  [21]. Fig. 1(b) displayed the PXRD patterns of the ZIF-L, where the sharp patterns confirmed the formation of ZIF-L with a high crystalline structure [22]. In the FT-IR spectra of ZIF-L, all the characteristic peaks were in excellent agreement with the reported literature (Fig. 1(c) [11,23]. Here, it noted that the peak assigned at  $424 \text{ cm}^{-1}$  demonstrates clear indications of the Zn-N nature of the synthesized ZIF-L. Thermogravimetric analysis (TGA), which was carried out under a nitrogen atmosphere, indicates the sufficient thermal stability of the synthesized ZIF-L for polymerization reactions (Fig. 1(d)). One reason for the weight loss of about 8.88 % before  $270 \text{ }^\circ\text{C}$  may be the removal of residual solvent from ZIF-L. However, it shows a very small amount of weight loss ( $<2.73 \%$ ) for water absorbed around  $100 \text{ }^\circ\text{C}$  [23]. Also, nitrogen sorption measurement was performed to get an idea about the microporous structure of ZIF-L (Fig. 1(e)). The corresponding shape falls in type I isotherm, indicating the microporous structure of the ZIF-L.



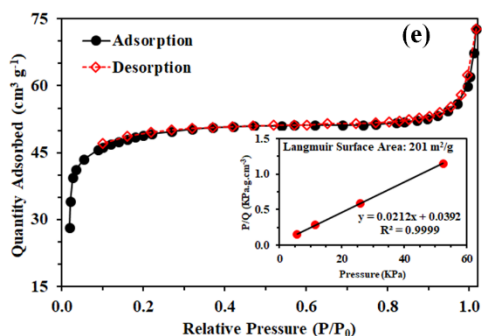


Fig. 1. Characterizations of the synthesized ZF-L: a) SEM image (scale 10  $\mu\text{m}$ ) which showed leaf-like nature; b) PXRD patterns, all sharp diffraction peaks show the characteristics of ZIF-L; c) FTIR spectrum; d) TGA curve determined under  $\text{N}_2$  atmosphere (20 mL/min) in the range of 30–600  $^\circ\text{C}$ ; and e) The nitrogen adsorption-desorption isotherms measured at 77K, the corresponding results were as follows: BET surface area of 176  $\text{m}^2 \text{g}^{-1}$ ; the total pore volume of 0.062  $\text{cm}^3 \text{g}^{-1}$ , respectively.

### 3.2. Block copolymerization of MMA and CL

Previously, we have reported a synthetic strategy for generating ultra-high molecular weight poly (methyl methacrylate) PMMA using ZIF-L as a robust catalyst [24]. The catalytic activity of ZIF-L is mainly responsible for its structural defects in open, active sites (active acidic and basic). Based on these polymerizations, we studied the copolymerization of MMA with CL by sequential addition using ZIF-L without any co-catalyst in a solvent-free medium at 140  $^\circ\text{C}$ . For this purpose, firstly, we have confirmed the successful formation of poly-caprolactone (PCL) following the homo polymerization of CL using ZIF-L. Also, no polymer was identified from the blank test, indicating the robust nature of ZIF-L for the copolymerization of MMA with CL. The synthesized copolymer was then characterized using common analytical techniques such as  $^1\text{H-NMR}$ ,  $^{13}\text{C-NMR}$ , GPC, DSC, and finally, ICP analysis. However, ensuring that we had block copolymers and not a mixture of two homo-polymers is important. Block copolymers were separated from homo-polymers by fractional precipitation methods for these purposes. The characteristic copolymerization conditions and results have been summarized in Table 1. In these circumstances, the number of active sites of ZIF-L (acidic and basic sites) was checked using the temperature program desorption (TPD) method. These results indicate the catalysts contain more acidic sites compared to their basic sites.

Table 1. Homo- and copolymerization of MMA with CL using ZIF-L at 140 °C without any co-catalyst in solvent-free medium<sup>a</sup>

Entry	Monomer		Polymer	Conv. <sup>g</sup> (%)		Yield <sup>h</sup> (mg)	$M_{n,GPC}$ <sup>i</sup> (kg/mol)	$\bar{D}$ <sup>i</sup>	$(\gamma_1 - \gamma_2)$
	$M_1$	$M_2$		$M_1$	$M_2$				
1 <sup>b</sup>	MMA		PMMA	72		329	919	1.81	2.5–3.8
2 <sup>b</sup>	CL		PCL	82		367	51	1.21	1.05–1.3
3 <sup>c</sup>	MMA	CL	PMMA- <i>b</i> -PCL	31	25	142	439	1.63	1.4–2.3
4 <sup>d</sup>	MMA	CL	PMMA- <i>b</i> -PCL	49	38	219	768	1.45	1.5–2.1
5 <sup>e</sup>	MMA	CL	PMMA- <i>b</i> -PCL	78	85	349	1190	1.40	1.5–2.2
6 <sup>f</sup>	MMA	CL	PMMA- <i>b</i> -PCL	77	83	338	1108	1.58	1.6–2.1

<sup>a</sup>[ $M_1$ ] = [ $M_2$ ] = 4.7 mM, [ZIF-L] = 0.047 mM, [monomer]/[ZIF-L] = 100; <sup>b</sup>reaction time: MMA = CL = 24 h; <sup>c</sup>reaction times: MMA (6 h) and CL (6 h); <sup>d</sup>reaction times: MMA (12 h) and CL (12 h); <sup>e</sup>reaction times: MMA (24 h) and CL (24 h); <sup>f</sup>using recovered ZIF-L (3<sup>rd</sup> cycle); <sup>g</sup>conv. = % of monomer conversion calculated by <sup>1</sup>H NMR spectroscopy in CDCl<sub>3</sub>; <sup>h</sup>Yield of polymer observed experimentally; <sup>i</sup>determined by gel permeation chromatography (GPC) analysis in THF at RT referenced to polystyrene standards.

To appraise the nature of polymers obtained by sequential addition of MMA and CL using ZIF-L catalysts, synthesized copolymers were tested by various conventional techniques such as <sup>1</sup>H-NMR, <sup>13</sup>C-NMR, GPC, DSC, ICP analysis, etc. In this continuity, Fig. 2(i) demonstrates the characteristic <sup>1</sup>H NMR spectra of the synthesized copolymer, PMMA-*b*-PCL, which confirms both monomers participated in this polymer formation. However, the results of <sup>13</sup>C-NMR spectroscopy provide evidence of block copolymer synthesis, in comparison with the spectra of PMMA and PCL homo-polymers, the characteristic peaks at 177.8 ppm (C=O in the MMA), 173.5 ppm (C=O of  $\epsilon$ -CL unit), 51.8 ppm (-OCH<sub>3</sub> in MMA unit) and 34.1 ppm (O=CCH<sub>2</sub>- in the  $\epsilon$ -CL unit) indicates block copolymer nature of the synthesized copolymer, as shown in Fig. 2(ii). The copolymer PMMA-*b*-PCL exhibits only one glass transition temperature ( $T_g$ ) like a single polymer, which reveals a good deal with the reported data. The  $T_g$  value of PMMA-*b*-PCL (16.6 °C) exists within that of their corresponding homo-polymers such as PMMA (122.4 °C) and PCL (-54.3 °C) (Fig. 3), confirming the presence of greater PMMA block in copolymer chain. Also, the melting temperature ( $T_m$ ) of PMMA-*b*-PCL was observed to be significantly lower, suggesting that the  $T_m$  value decreases due to the increase in the disorder of the polymeric segment, along with the crystallinity (Table 2) [25]. Thus, the NMR and DSC results indicate that CL and MMA segments formed block copolymers using ZIF-L.

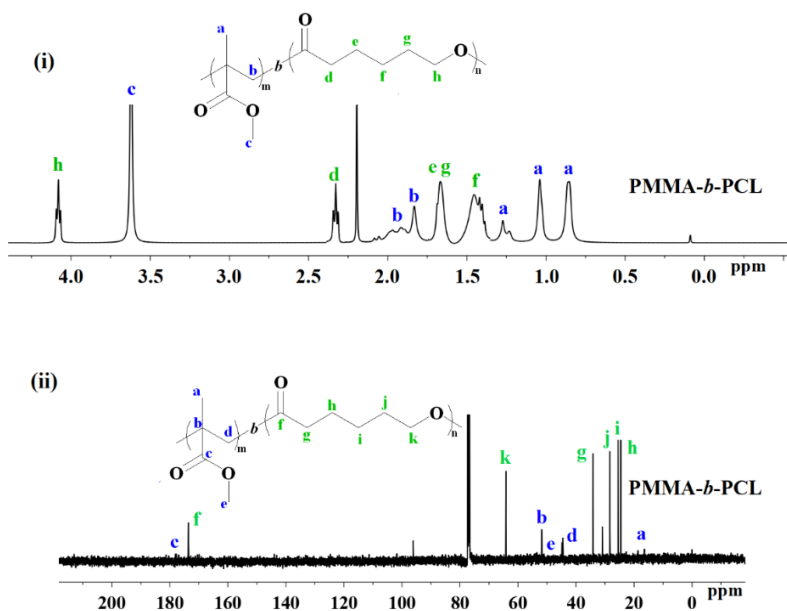


Fig. 2. (i)  $^1\text{H}$ -NMR and (ii)  $^{13}\text{C}$ -NMR spectrum in  $\text{CDCl}_3$  of PMMA-*b*-PCL copolymer synthesized using ZIF-L (Table 1, entry 5).

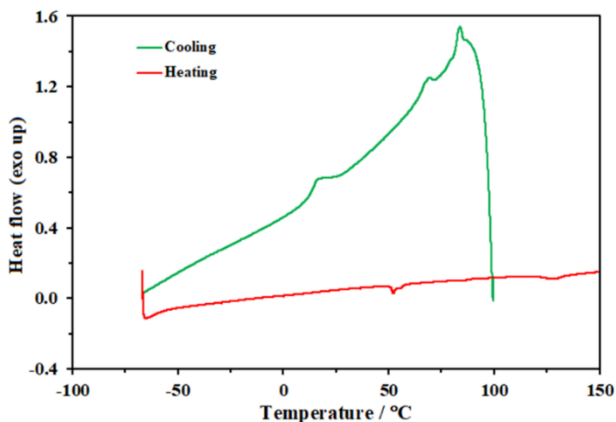


Fig. 3. DSC curves of copolymer PMMA-*b*-PCL (Table 1, entry 5): cooling scans (green) and subsequent heating scans (red).

Table 2. Thermal properties of block copolymer PMMA-*b*-PCL with their homo-polymers PMMA and PCL.

Polymeric Sample	$T_g$ (°C)	$T_m$ (°C)
PMMA	122.4	289
PCL	- 54.3	56.8
PMMA- <i>b</i> -PCL <sup>a</sup>	16.6	61.5

<sup>a</sup> Table 1; entry 5

The GPC traces of the synthesized copolymer PMMA-*b*-PCL show a mono-modal molecular weight distribution similar to that of their corresponding homo-polymers, that are in good agreement with the various reported values of block polymer following the same monomers (Fig. 4) [26]. In addition, the fractional precipitation method is a suitable method, indicating the formation of block copolymer (Fig. 5) [20,25,27]. In the THF-methanol system, the  $\gamma$  values for PMMA-*b*-PCL copolymer were observed in between those of their corresponding homo-polymers, confirming the formation of block copolymer (Table 1).

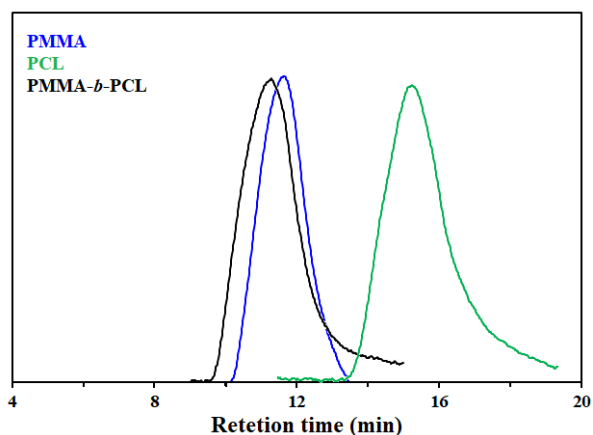


Fig. 4. GPC trace of block copolymer PMMA-*b*-PCL with their homo-polymers PMMA and PCL shown for comparison.

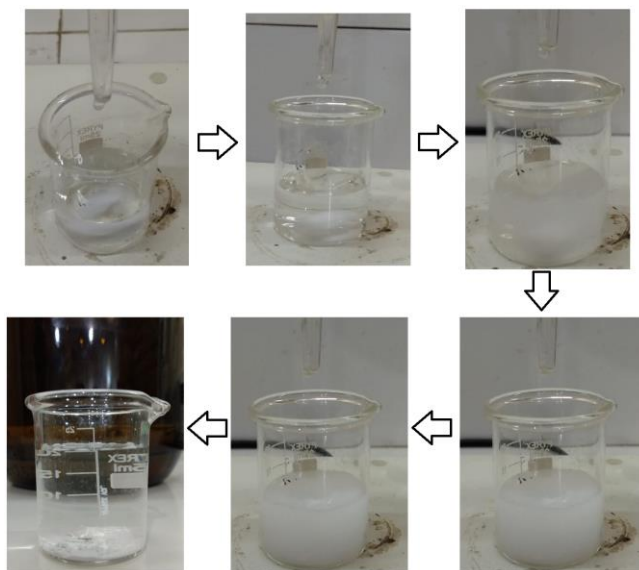
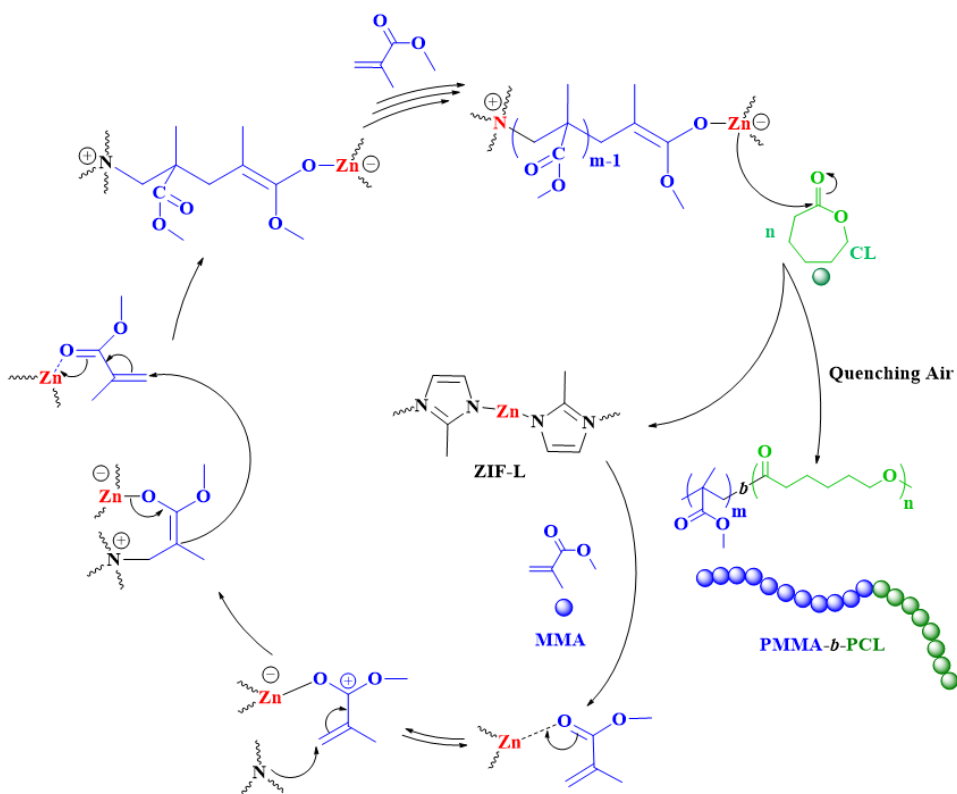


Fig. 5. Fractional precipitation method for the separation of block copolymers from their corresponding homo-polymers.

Considering the structure of ZIF-L, its reactivity, and the results of the current studies, we propose the block copolymerization mechanism of MMA and CL (Scheme 2). Although the proposed scheme does not reveal all the details of copolymerization, we can get a general idea about the block copolymerization mechanism from it. In this polymerization process, we have used sequential addition of monomer (MMA is first added), so we suggest that the polymerization proceeds through the activation in a cooperative (Lewis acid and base sites) manner of ZIF-L [24]. Lewis acid sites initiate the chain propagation in this part, forming Zwitterion-type intermediates. However, after the addition of CL to the system at the inert medium, the polymerization proceeds in the nucleophilic attack of the carbonyl group of CL, followed by the ROP to form block copolymers [28].



Scheme 2. Proposed mechanism for the synthesis of copolymer PMMA-*b*-PCL using ZIF-L.

Since there is a relationship between the stability and catalytic performance of heterogeneous catalysts, we have tested the recoverability and reusability of ZIF-L at these stages. The results of PXRD, and SEM (Fig. 6) before and after copolymerization give an idea of catalyst stability. The results confirmed that the catalyst ZIF-L is stable enough even after using it at least three times for polymerization, although very little leaching of zinc metal has occurred into the mixture. After that, we reused the recovered

ZIF-L to investigate the catalytic activity under identical conditions (Table 1, entry 6). The results demonstrated in the table suggest that the catalyst ZIF-L can retain its catalytic activity with no significant loss in activity.

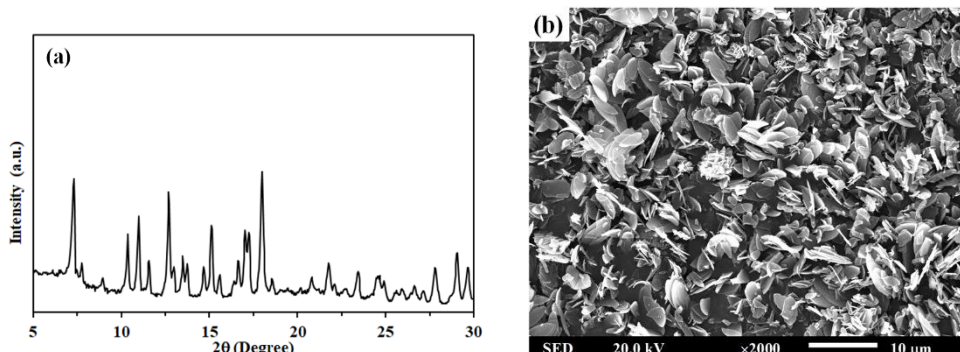


Fig. 6. (a) PXRD and (b) SEM image of the recovered (after use 3<sup>rd</sup> cycle) ZIF-L.

## Conclusion

In conclusion, we have successfully synthesized the high molecular weight block copolymer of MMA with CL following the simple sequential addition of monomers without any co-catalyst in a solvent-free medium, and in this process, ZIF-L is used as a robust polymerization catalyst. Various characterization techniques (<sup>1</sup>H-NMR, <sup>13</sup>C-NMR, GPC, DSC, fractional precipitation techniques) were used to identify the nature of the synthesized polymer, and the results proved that the resulting copolymer has a block polymer structure. Our proposed mechanistic studies suggest that the acidic sites of ZIF-L initiate the polymerization reaction by forming a Zwitterion-type intermediate, which can then initiate CL polymerization through nucleophilic invasion of the CL carbonyl group.

## Acknowledgments

The authors are grateful to the University Grants Commission of Bangladesh (UGCB) - Mawlana Bhashani Science and Technology University for financial support. M.A.R. would like to thank F. Verpoort, Laboratory of Organometallics, Catalysis and Ordered Materials, Wuhan University of Technology, Wuhan 430070, China, for cordial support.

## References

1. M. Zhao, Q. Lu, Q. Ma, and H. Zhang, *Small Methods* **1**, 1600030 (2017).  
<https://doi.org/10.1002/smt.201600030>
2. S. Mochizuki, T. Kitao, and T. Uemura, *Chem. Commun.* **54**, 11848 (2018).  
<https://doi.org/10.1039/C8CC06415F>
3. T. A. Goetjen, J. Liu, Y. Wu, J. Sui, X. Zhang et al., *Chem. Commun.* **56**, 10409 (2020).  
<https://doi.org/10.1039/D0CC03790G>

4. A. Bavykina, N. Kolobov, I. S. Khan, J. A. Bau, A. Ramirez, and J. Gascon, *Chem. Rev.* **120**, 8468 (2020). <https://doi.org/10.1021/acs.chemrev.9b00685>
5. C. Yang, W. Zhang, J. Wang, S. Li, X. Liu et al., *Inor. Chem Front.* **6**, 2667 (2019). <https://doi.org/10.1039/C9QI00851A>
6. B. Chen, Z. Yang, Y. Zhu, and Y. Xia, *J. Mater. Chem. A* **2**, 16811 (2014). <https://doi.org/10.1039/C4TA02984D>
7. A. Zanon and F. Verpoort, *Coordi. Chem. Rev.* **353**, 201 (2017). <https://doi.org/10.1016/j.ccr.2017.09.030>
8. R. Chen, J. Yao, Q. Gu, S. Smeets, C. Baerlocher et al., *Chem. Commun.* **49**, 9500 (2013). <https://doi.org/10.1039/C3CC44342F>
9. T. Wang, Z. Kou, S. Mu, J. Liu, D. He et al., *Adv. Funct. Mater.* **28**, ID 1705048 (2018). <https://doi.org/10.1002/adfm.201705048>
10. Y. Feng, H. Wang, and J. Yao, *Coordi. Chem. Rev.* **431**, ID 213677 (2021). <https://doi.org/10.1016/j.ccr.2020.213677>
11. Z.-X. Low, J. Yao, Q. Liu, M. He, Z. Wang et al. *Cryst. Growth Des.* **14**, 6589 (2014). <https://doi.org/10.1021/cg501502r>
12. W. N. Ottou, E. Conde-Mendizabal, A. Pascual, A. -L. Wirotius, D. Bourichon et al., *Macromolecules* **50**, 762 (2017). <https://doi.org/10.1021/acs.macromol.6b02205>
13. V. Hasirci and N. Hasirci, *Fundamentals of Biomaterials* (Springer, Switzerland, 2018).
14. S. K. Prajapati, A. Jain, A. Jain, and S. Jain, *Eur. Polym. J.* **120**, 109191 (2019). <https://doi.org/10.1016/j.eurpolymj.2019.08.018>
15. X. Li, C. Chen, and J. Wu, *Molecules* **23**, 189 (2018). <https://doi.org/10.3390/molecules23010189>
16. L. S. Nair and C. T. Laurencin, *Prog. Polym. Sci.* **32**, 762 (2007). <https://doi.org/10.1016/j.progpolymsci.2007.05.017>
17. A. Bettencourt and A. J. Almeida, *J. Microencapsul.* **29**, 353 (2012). <https://doi.org/10.3109/02652048.2011.651500>
18. H. Yang, J. Xu, S. Pispas, and G. Zhang, *Macromolecules* **45**, 3312 (2012). <https://doi.org/10.1021/ma300291q>
19. T. Öztürk, M. Yavuz, M. Gökteş, and B. Hazer, *Polym. Bull.* **73**, 1497 (2016). <https://doi.org/10.1007/s00289-015-1558-2>
20. B. Wu, R. W. Lenz, and B. Hazer, *Macromolecules* **32**, 6856 (1999). <https://doi.org/10.1021/ma990166o>
21. G. Liu, Z. Jiang, K. Cao, S. Nair, X. Cheng et al., *J. Membrane Sci.* **523**, 185 (2017). <https://doi.org/10.1016/j.memsci.2016.09.064>
22. Z. Zhong, J. Yao, R. Chen, Z. Low, M. He et al., *J. Mater. Chem. A* **3**, 15715 (2015). <https://doi.org/10.1039/C5TA03707G>
23. B. Ding, X. Wang, Y. Xu, S. Feng, Y. Ding et al., *J. Colloid Interf. Sci.* **519**, 38 (2018). <https://doi.org/10.1016/j.jcis.2018.02.047>
24. M. A. Rahaman, B. Mousavi, F. Naz, and F. Verpoort, *Catalysts* **12**, 521 (2022). <https://doi.org/10.3390/catal12050521>
25. H. -J. Jung, I. Yu, K. Nyamayaro, and P. Mehrkhodavandi, *ACS Catal.* **10**, 6488 (2020). <https://doi.org/10.1021/acscatal.0c01365>
26. X. -H. Liu, Q. -Y. Zhang, W. -I. Di, Y. -G. Zhang, and C. Ding, *Polym. Chem.* **8**, 4752 (2017). <https://doi.org/10.1039/C7PY01040K>
27. T. Öztürk, M. Gökteş, and B. Hazer, *J. Macromol. Sci. A* **48**, 65 (2010). <https://doi.org/10.1080/10601325.2011.528310>
28. Q. Wang, W. Zhao, J. He, Y. Zhang, and E. Y. X. Chen, *Macromolecules* **50**, 123 (2017). <https://doi.org/10.1021/acs.macromol.6b02398>